

# Longitudinal electrical resistivity profiles for non-destructive tree trunks inspection

Vinicius Rafael Neris dos Santos<sup>1\*</sup>, Bruno Araújo Furtado de Mendonça<sup>2</sup>,  
João Vicente de Figueiredo Latorraca<sup>3</sup>, Marcelo Farias Caetano<sup>4</sup>

<sup>1</sup>University of São Paulo, 'Luiz de Queiroz' College of Agriculture, Department of Forest Sciences, Piracicaba, SP, Brazil

<sup>2</sup>Federal Rural University of Rio de Janeiro, Campus of Seropédica, Forestry Institute, Department of Silviculture, Seropédica, RJ, Brazil

<sup>3</sup>Federal Rural University of Rio de Janeiro, Campus of Seropédica, Forestry Institute, Department of Forest Products, Seropédica, RJ, Brazil

<sup>4</sup>University of São Paulo, Institute of Mathematics and Statistics, Department of Applied Mathematics, São Paulo, SP, Brazil

## TECHNOLOGY OF FOREST PRODUCTS

### ABSTRACT

**Background:** The development and application of new technologies and solutions are extremely important to manage and monitor urban forestry to prevent accidents resulting from falls that often result in social and property damage. To evaluate the internal conditions of a tree, it is recommended to use indirect methods, both for the trunk and the root system. However, existing methods can predict trunk properties at the lower level in some situations, that can lead to a misinterpretation of the actual phytosanitary status of the evaluated specimen and cause the incomplete assessment. Thus, the present work aimed to evaluate, with acquisition and software development, the use of geophysical method of electrical resistivity (ER), with longitudinal profiles along the trunk, every 45°, for internal and non-destructive analysis of two specimens of *Eucalyptus sp.* and one of *Pachira aquatica* trees. In these trees, data were acquired and compared each other's by ER, mechanical impulse tomography and resistograph.

**Results:** This approach allows for the investigation the entire length of the trunk, in a reduced time. From the results, it was possible to establish qualitative (from images) and some quantitative (physical property values) relationships between the ER, impulse tomography and resistography, by the internal image generated and the physical properties obtained.

**Conclusion:** Both in the interpretation of the generated images and the values obtained, they exhibited different characteristics of the studied wood, demonstrating the potential of the developed methodology for rapid and precise application in urban trees.

**Keywords:** Electrical resistivity; Non-destructive evaluation; Resistograph; Sonic tomography.

### HIGHLIGHTS

Development of new technologies is important to manage and monitor urban forestry.  
New methodology for monitoring urban forestry to avoid accidents.  
New approach with longitudinal profiles along the trunk of electrical resistivity data.  
Experiments in laboratory scale and with two different species.

SANTOS, V. R. N.; MENDONÇA, B. A. F.; LATORRACA, J. V. F.; CAETANO, M. F. Longitudinal electrical resistivity profiles for non-destructive tree trunks inspection. CERNE, v.31, e-103426, 2025. doi: 10.1590/01047760202531013426.

## INTRODUCTION

In Brazil, especially in large cities, it is common for urban expansion to occur in a disorderly manner, with little or no planning (Carvalho et al., 2023; Cavalari et al. 2024). In this context, the implementation and/or monitoring of urban green areas are priorities, in which trees in an urban environment can guarantee the maintenance of their functionality (Grote et al. 2016; Rahman et al. 2018). Thus, the development and application of new technologies aimed at maintaining and managing urban trees are extremely important to prevent accidents resulting from falls, often resulting in social and property damage and even loss of life.

It is well known that urban afforestation brings several benefits to the environment and human health: increased soil permeability; air temperature and humidity control; reduction of noise and atmospheric pollution; psychological well-being and habitat for birds and other faunal species (Vogt et al. 2017). However, due to faulty planning, the choice of the species to be planted on public roads is sometimes made incorrectly, resulting in conflicts with the existing infrastructure (*Secretaria Municipal do Verde e do Meio Ambiente* 2015; Cunha et al. 2020).

Assessing the stability of trees is an indispensable tool for preserving the integrity of people and properties in the urban context of cities (Santos & Teixeira, 2001). Therefore, it is necessary to know the studied species, their physical, chemical and biological properties, as well as the way they relate to the environment in which they are inserted and with the investigation methods available.

Currently, there are several methods used in the evaluation of trees, including mechanical impulse tomographs in the trunk or roots (Guardia, 2020; Dudkiewicz & Durlak, 2021; Fu et al. 2024) and electrical resistance (Divaskara & Chaithra, 2022), pulling test (Todo et al. 2022) and penetrometer, resistograph or increment auger (Papandrea et al. 2022; Kantavichai & Turnblom, 2022). These methods differ from each other by the evaluated physical properties, execution time, resolution of the results, cost and degree of invasion. In Brazil, impulse tomograph and resistograph technologies have become a reference in decision-making for tree management in urban forests, most of which are carried out on trunks (Emerick, 2021).

Recent works have been published using alternative methodologies to those applied today, such as Santos et al. (2022) who used the GPR method for three-dimensional mapping of the roots of a *Libidibia ferrea* tree. Apaydin et al. (2022), applied GPR to improve the internal imaging of tree trunks through numerical simulations and controlled experiments in the laboratory and Feng et al. (2023) used the geophysical inversion technique of GPR data to image the internal structure of tree trunks. The use of electrical resistivity in forestry studies is still incipient, being more applied in works to map roots in soil (Ehosioko et al. 2020; Balawant et al. 2022) or detect wood decay (Hagrey, 2006; Soge et al. 2019). In this context, the present work aimed to evaluate the applicability of the geophysical method of electrical resistivity (ER), with a new approach of longitudinal

profiles along the trunk, in the evaluation of the internal structure of tree trunks and to determine differences in electrical resistivity values between the analyzed species, as well as for the internal injuries of the trunks, correlating them with the results of mechanical impulse tomography (propagation velocity) and resistography (resistance to drill penetration).

## MATERIAL AND METHODS

### Electrical resistivity method (ER)

Geoelectric methods aim to determine the distribution of some electrical physical parameters in the subsurface through surface measurements. The electrical resistivity method uses the apparent electrical resistivity to characterize a material or medium, a magnitude that is related to the mechanisms of propagation of electrical currents in them. Basically, electrical resistivity quantifies the resistance that a given material offers to the passage of electric currents, as well as its inverse parameter, conductivity, quantifies the ease that a material must transmit current inside it, that is, allow its passage. According to Telford et al. (1990), if we consider a cylindrical body made of homogeneous and conductive material, with length  $L$  and cross section  $S$ , we can define its theoretical resistivity ( $\rho$ ), according to Equation 1.

$$\rho = \frac{R \cdot S}{L} \quad (1)$$

with  $R$  being the electrical resistance (Ohm). When crossed by an electric current ( $I$ ), the cylinder will be subjected to an electric potential difference ( $\Delta V$ ) and its resistance will be (Ohm's Law), according to Equation 2.

$$R = \frac{\Delta V}{I} \rightarrow \rho = \frac{\Delta V S}{I L} \quad (2)$$

Unlike resistance ( $R$ ), electrical resistivity is a very specific magnitude of materials, depending on their intrinsic microscopic characteristics, which make them good tools for diagnosing a medium, such as tree trunks, for example. The water and dissolved salt contents are the most important, and their increase is inversely proportional to the resistivity. This physical property can present, therefore, a great variation of values, which increases its applicability in studies of different natures, such as hydrogeological, environmental and in the application suggested in this work, in the detection of cavities and internal injuries of tree trunks.

The electrical resistivity method is applied introducing an artificial electric current in the medium (trunk), through two electrodes (conventionally called current electrodes, "A" and "B") and the potential generated in two other electrodes located in the proximity to the current flow (potential electrodes, "M" and "N"), which

will allow calculating the real or apparent resistivity of the medium (Orellana, 1972; Telford *et al.* 1990; Reynolds, 1997). The electrical resistivity (in *Ohm.m* or  $\Omega m$ ) depends on the injected current, the potential difference measured between MN electrodes and the arrangement geometry, called the geometric factor (*K*), according to Equation 3.

$$\rho = \frac{\Delta V_{MN}}{I} K \quad (3)$$

The array chosen for measurements in trunks was the dipole-dipole, where the spacing *a* between the pair of current electrodes (AB) is the same of potential electrodes (MN) pair and the distance between these two pairs is 'na' factor. After carrying out the first measurement, a pair of electrodes is moved forward a distance 'na', thus increasing the depth of investigation. The geometric factor for the dipole-dipole array is given by Equation 4.

$$K = \pi n(n+1)(n+2)a \quad (4)$$

### Sonic tomography

Sonic or mechanical impulse tomography is based on measuring the travel times of mechanical waves (Rust & Göcke, 2000; Burcham *et al.*, 2023). Impulse velocities within wood are highly correlated with the density of the material and therefore can be used to gather information about its quality. Dense healthy wood transmits stress waves better than damaged wood by decay or cracking.

Each sensor is equipped with a vibration meter capable of performing direct real-time analysis of incoming pulses. By producing a vibration in the sensors, with a hammer for example, it generates stress waves that travel through the wood. The time that the stress waves travel between the sensors is recorded and converted into velocities. According to Smulski (1991), the propagation velocity (*v*) of the mechanical wave is directly proportional to the square root of the elastic modulus (*E*) of the wood and inversely proportional to the square root of its density (*d*), according to Equation 5.

$$v = \sqrt{\frac{E}{d}} \quad (5)$$

The propagation velocity of mechanical waves will be greater in wood of greater density, since the predominant factor is the elastic modulus, which is the physical property that can change with the decay of the wood (Deflorio *et al.* 2008).

Although sonic tomography is already widespread worldwide, like any indirect method, it presents ambiguities in the results for some specific cases of internal trunk injury. According to Göcke *et al.* (2008) some types of defects can cause the same image in tomography, circular or radial cracks

and cavities can indicate the same result in the tomographic image and for this reason it is recommended to apply all the knowledge about typical defects in trees, as well as the operation of the tomograph for a correct evaluation, in addition to the use of other tools for the obtaining additional information.

### Resistograph

The resistograph is a mechanical resistance measurement device, developed by Frank Rinn in 1986, for tree inspection. The equipment drives a needle with 1.5 mm of diameter into the wood and measures the drill resistance as it rotates (Rinn *et al.*, 1996). The drill resistance is concentrated at the tip of the needle and an electronic regulation of the motor guarantees a constant feed rate adapted individually to the wood density (Rinn, 1994).

The resistograph is a specialized tool used in tree risk assessment to evaluate internal structural integrity of trees, particularly to detect decay, cavities, and other wood density variations (Suchocka *et al.*, 2023). It provides detailed and precise measurements, making it possible to distinguish between healthy wood, partially decay wood, and completely decayed or hollow areas.

### Controlled tests

Initially, experiments were carried out to determine the best ways to acquire geophysical data for electrical resistivity in trunks, as well as a preliminary evaluation of the data reading and image generation program. A PVC tube of 2.0 m high and 20 cm in diameter was used, filled with slightly moistened sand in an inhomogeneous way (Figure 1). This scheme was chosen because it is a cylindrical medium and the use of wet sand aims to simulate additional anomalies inside the tube, like what can be found inside the tree trunk. In the upper right quadrant, another PVC tube was inserted, however, empty (or filled with air), 2.0 m of high and 5 cm in diameter, simulating a cavity (diagram in Figure 1a).

Several acquisition modes were tested to obtain the best relationship between quality, resolution and acquisition time. To obtain the data, we opted for longitudinal profiles (Figure 1b), emulating the way in which the equipment is used in its original design and, in this way, obtaining data that is more credible with reality. It is noteworthy that in a single data acquisition with the ER method it is already possible to obtain results at different heights, that is, once the maximum height is defined, the entire "cylinder" is investigated.

For data acquisition with ER, the dipole-dipole arrangement was used, with 10 cm spacing between electrodes (stainless steel nail). To optimize data collection, profiles were defined at every 45°, all around the tube resulting in eight longitudinal profiles, where this interval can vary according to the tree diameter (DBH – diameter at breast height) or the desired resolution for the results. To visualize the results, a script was developed in Python language that processes, organizes, and plots the sections at heights determined by the user (Santos *et al.* 2022), through a 3D data interpolation. The result of the experiments can be seen in Figure 1c, in a cross section of the PVC tube at a height of 1.0 m.

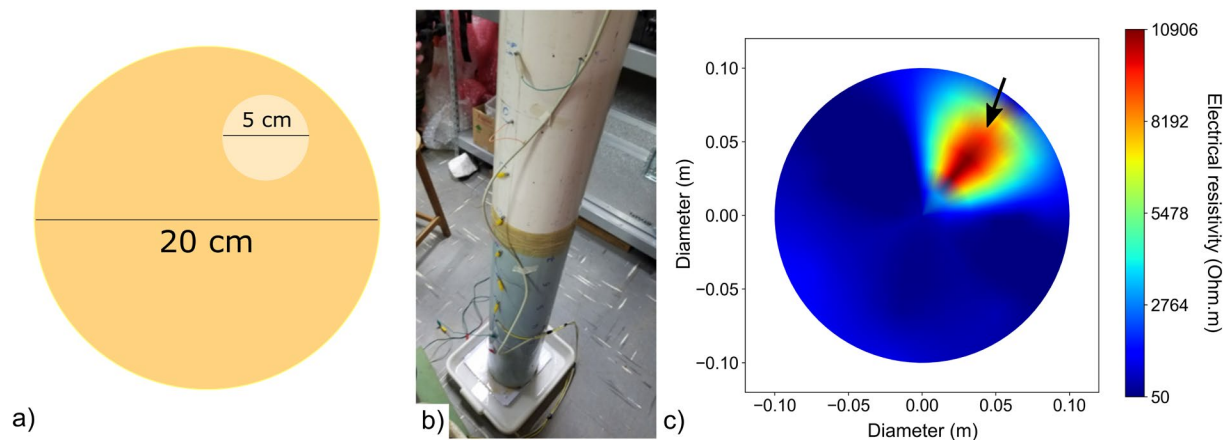


**Figure 1:** PVC tube experiments. a) Tubes dimensions. b) Electrical resistivity acquisition data. c) Experimental results (black arrow: empty PVC tube position).

From the generated image, it was possible to detect the position of the empty pipe (black arrow), with high electrical resistivity values (approximately 11,000  $\Omega\text{m}$ , in red), as it is filled with air. With the electrical method it is also possible to identify regions with higher humidity (low electrical resistivity, in darker blue). An important point that must be considered is that, in the way it was implemented, the methodology does not provide the exact size or geometry of the target found, making it possible to locate its influence region.

### Tree trunks data acquisition

After the validation carried out from the experiments in the PVC tube, data were collected in the field on three different trees, two examples of *Eucalyptus sp.* and one *Pachira Aquatica* (popularly called 'munguba' in Brazil). The trees are located at the Campus of the Federal Rural University of Rio de Janeiro (UFRRJ), in Seropédica city, Brazil. *Eucalyptus sp.* is a plant of the *Myrtaceae* family, which are native to Oceania and include more than 700 different species. It has commercial value, since it is used for energy, cellulose and paper and sawmill. The most important feature for the present study is the basic density, with values ranging from 450 to 980  $\text{kg}/\text{m}^3$  (Nowak, 2021). The *Pachira aquatica* belongs to the *Malvaceae* or *Bombacaceae* family, originates in Central and South America. Its wood is very light and whitish, with densities ranging from 380 to 430  $\text{kg}/\text{m}^3$  (Nowak, 2021; Cruz, 2022).

The choice for these two species was due to the great difference in wood density, a determining factor for the propagation of mechanical waves and it was expected to relate the velocities found by the tomography with the electrical resistivity of the ER method, in addition to confirming some anomalous region through the resistograph. The selected eucalyptus trees, called EU1 and EU2, with DBH of 0.78 m and 0.67 m, respectively, with EU1 having a normal visual appearance, with no apparent defects and EU2 having little crown coverage, with some apparent defects at its base.

The selected 'munguba', MG1, with DBH of 0.76 m, generally presents a good visual condition and a leafy crown.

Arbotom equipment, from the manufacturer Rinntech, was used with eight sensors arranged at every 45° in the trunk circumference (Figure 2a). Velocity sections were acquired at the tree base and height of the DBH (1.30 m) of the trees. For a more assertive assessment and to reduce ambiguities in the internal state of the analyzed trunks, a resistograph was used (direct method), which measures the wood's resistance to drill penetration (in percentage) as a function of the drill's entry distance. The resistograph used was from Rinntech, model 4452-S with a 1.5 mm diameter drill (Figure 2b). The perforation sites were defined from the images generated by the mechanical impulse tomograph, where some type of variation in the propagation velocity was observed.

Electrical resistivity data were collected with the Syscal Pro equipment, from the manufacturer Iris Instruments, with a dipole-dipole array, nine channels (dipoles) and electrode spacing of 15 cm (Figure 2c). The profiles started at the tree base and went up to a height of 1.60 m, in the same positions as the tomograph sensors. The data were pre-processed to obtain the electrical resistivity profiles and then they are organized and visualized by the developed script, through cross sections at different heights, depending on the distribution of electrical resistivity inside the trunk.

## RESULTS

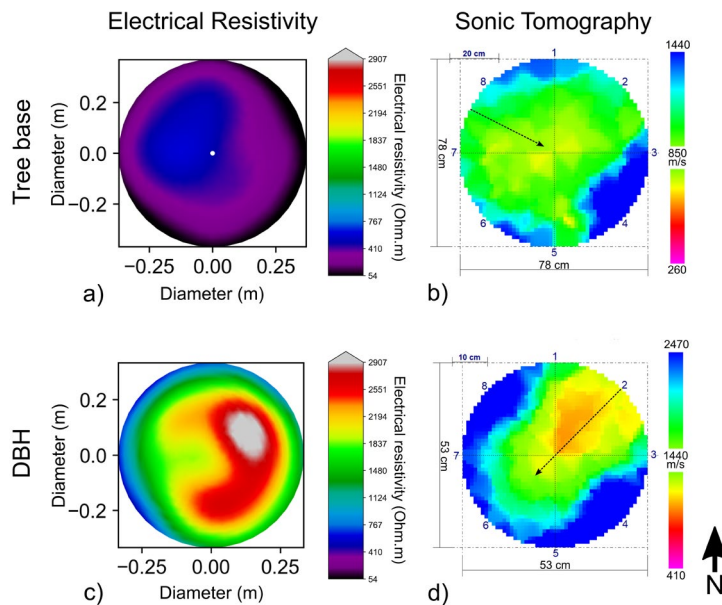
In the results, the tomography sections show the variation of velocities (m/s) of the mechanical wave inside it, whereas the electrical resistivity (ER) method presents the distribution of electrical resistivity ( $\Omega\text{m}$ ). The dashed arrows in the figures indicate the position, direction and length of the analysis performed by the resistograph, based on the tomographic images during the field works. The number of measurements was defined by the anomalies present in the tomography. In the absence of these anomalies, only one measurement was performed to verify the real integrity of the wood.

Figure 3 shows the comparison of the results obtained with ER and sonic tomography, at the tree base and DBH. The resistivity varied between 54 and 2907  $\Omega\text{m}$ , and the peripheral region can be interpreted by the sapwood region, presenting the lowest values (between 54 and 400  $\Omega\text{m}$ , black-purple region), indicating consistency with the presence of fluids, i.e., low resistivity.

At the tree base (Figure 3a) showed lower values in the live bark regions of the trunk, with emphasis on a central region (heartwood) with slightly higher resistivity. For the tomography, the maximum acoustic velocity found was 1440 m/s, predominating a region of the wood with values of 850 m/s (Figure 4b), not indicating any type of internal injury or decay. At the height of DBH, the electrical resistivity



**Figure 2:** Data acquisition with proposed methodologies. a) Mechanical impulse tomograph. b) Resistograph. c) Electrical resistivity.



**Figure 3:** Comparison between ER and tomograph of eucalyptus EU1, for the tree base at 0.10 m height and at the DBH at 1.30 m height (black dashed arrow: resistograph position and direction). a) Electrical resistivity at the tree base. b) Sonic tomography at the tree base. c) Electrical resistivity in the DBH. d) Sonic tomography in the DBH.

values (Figure 3c) showed the highest resistivities in the core of the trunk, higher than 2000  $\Omega\text{m}$ , corresponding to a drier material, little permeable, ancient and lacking living cells (Larsson *et al.*, 2004), while the tomography showed a region of low propagation velocity in position 2, in the amount of 1100 m/s, where the maximum value was 2470 m/s (Figure 3d). It is worth highlighting the coincidence of the images obtained for the DBH, as both methods showed a region of contrast in position 2 (point of investigation with the resistograph), for the ER in red/white and for the tomography in orange/red tones.

To verify the results found by the ER and tomography, an investigation was carried out with the resistograph, between points 7 and 8, at the tree base and at point 2, in the DBH region. Figure 4 shows the comparison between penetration resistance of resistograph drill (%) and electrical resistivity found, in the same position, at the tree base (Figure 4a – position 7-8) and at DBH (Figure 4d – position 2). In Figures 4b-4c and 4e-4f it is possible to see the overlap between the selected anomalous regions of electrical resistivity and sonic tomography and the resistographic amplitudes. The straight dashed line in these figures corresponds to the mean value ( $\mu$ ) of the amplitudes.

For the base, the two curves show an upward trend with increasing distance (bark-heartwood), with resistance reaching 60% and resistivity reaching the value of 400  $\Omega\text{m}$ , with mean value of 39%. A region between 5 and 10 cm stands out with a sharp decrease in resistance (10%), which coincides with the color transition between purple and blue in the ER

(Figure 4b), but a small variation of values, between 400 e 600  $\Omega\text{m}$ . The sonic tomograph did not show any significant variation with the resistography analysis (Figure 4c).

For the DBH (Figure 4d), the curves also show an upward trend with increasing distance, and the presence of a region between 10 and 25 cm, approximately, where the resistance to penetration decreases from 60% to 30% and the electrical resistivity presents its maximum peak, with 2100  $\Omega\text{m}$ . This region can be interpreted as a more friable and drier material (beginning of hollow, for example), which facilitates the entry of the drill and increases the measured resistivity and in this same region there was a decrease in the velocity propagation of the mechanical wave shown by the tomograph. The Pcc was 0.63, showing a good correlation too. By the overlapping the images and resistograph amplitudes (Figures 4e and 4f), it is possible to verify the agreement between the anomalous region (high electrical resistivity and low velocity) and the decrease in amplitude, with mean value of 38%, quite consistent with the tree basis region.

Figure 5 shows the comparison of the results found with electrical resistivity and sonic tomography, for the base and DBH, in eucalyptus EU2. The ER varied between 23 and 700  $\Omega\text{m}$  (Figure 5a) and position 1 highlights an increase in the physical property (in green), which coincides with the presence of a low wave propagation velocity of approximately 450 m/s (Figure 5b). Similarly, between positions 8 and 1, in the central region of DBH, with high values of electrical resistivity, greater than 610  $\Omega\text{m}$  (Figure 5c), and a low velocity, of 600 m/s (Figure 5d).

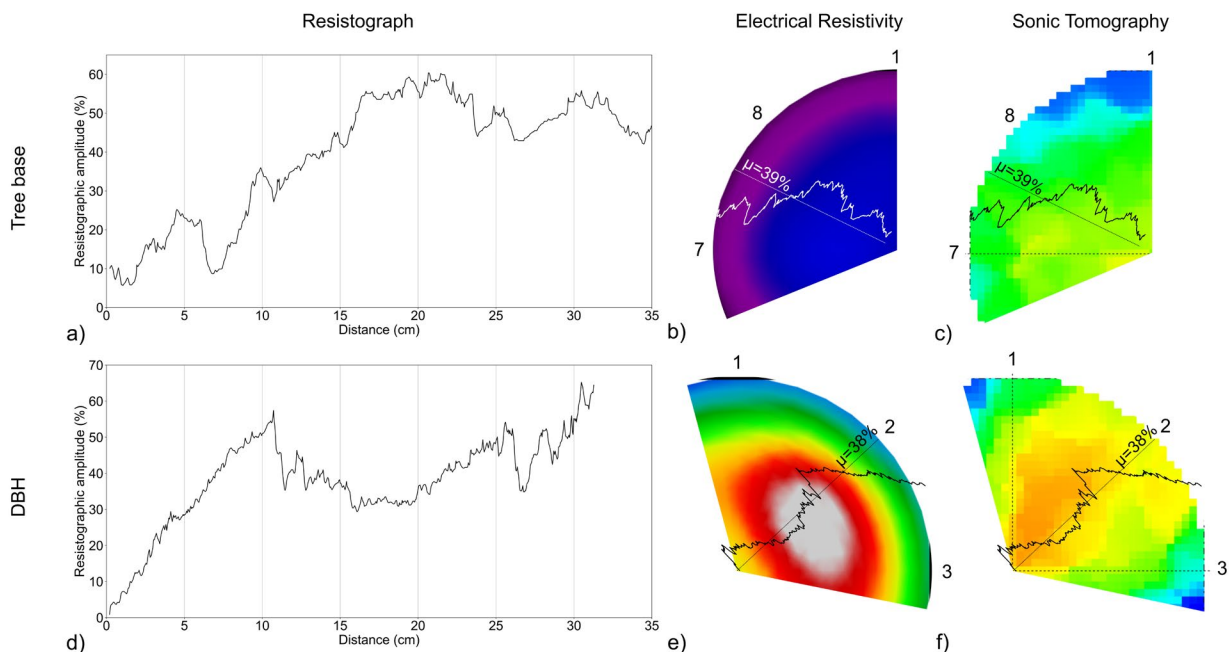


**Figure 4:** Resistograph results in eucalyptus EU1 compared with electrical resistivity and sonic tomography. a) Resistograph amplitudes between points 7 and 8, at the tree base. b) Overlap between electrical resistivity and resistographic amplitudes for the tree base. c) Overlap between sonic tomography and resistographic amplitudes for the tree base. d) Resistograph amplitudes in position 2, at the DBH. e) Overlap between electrical resistivity and resistographic amplitudes for the DBH. f) Overlap between sonic tomography and resistographic amplitudes for the DBH.

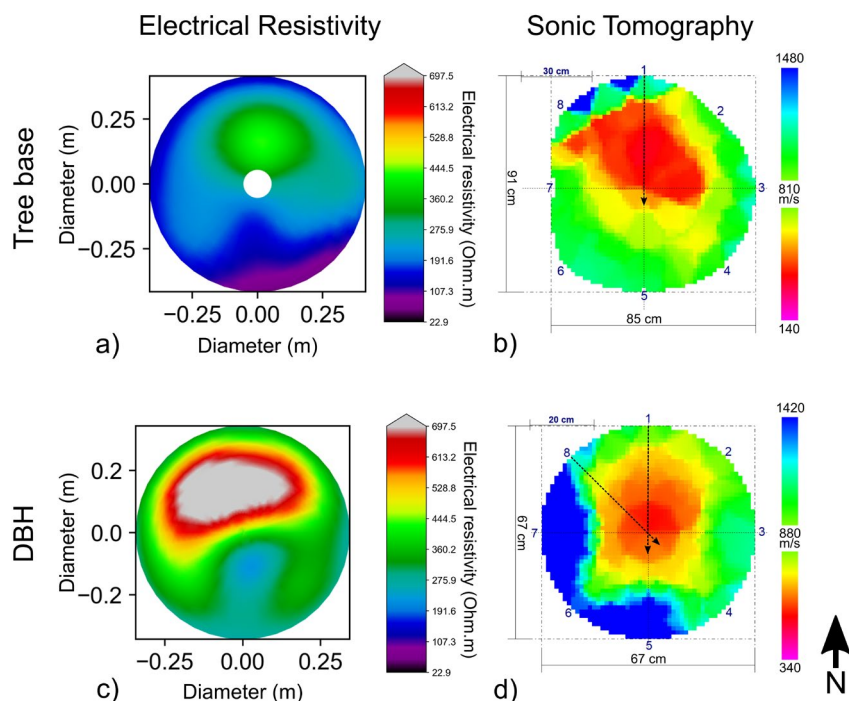


**Figure 5:** Comparison between ER and tomograph of eucalyptus EU2, for the tree base at 0.10 m height and at the DBH at 1.30 m height (black dashed arrow: resistograph position and direction). a) Electrical resistivity at the tree base. b) Sonic tomography at the tree base. c) Electrical resistivity in the DBH. d) Sonic tomography in the DBH.

In the regions highlighted by the tomography, in the same way, analyzes were performed with the resistograph (Figure 6), at position 1 at the tree base and at positions 1 and 8 at the DBH. The tree base region appears to be more compromised (Figure 6a), with maximum resistance values reaching approximately 30%, with many variations along the drill entry distance. The electrical resistivity values show an upward trend on the curve, with values greater than 250  $\Omega$ m. Between 5 and 15 cm the resistance drops to 7%, but there was no change in resistivity.

In DBH, the resistance to penetration reached values of 40% (position 1 – Figure 6d) and 50% (position 8 – Figure 6g) and showing variations along the distance, with both resistivity curves increasing. For this data set, at the tree base and DBH position 1, the electrical method not having sufficient resolution to detect small internal variations in the wood, as can be seen by the resistograph.

In the overlap results, despite the large variation in the resistograph amplitudes, there is agreement between the curves and the images. At the base of the tree (Figures 6b and 6c), position 1, the transition region between 200 and 300  $\Omega$ m, in the ER, and 800 and 400 m/s, in the tomography, approximately, presents a significant decrease in the resistograph, falling to 7% the amplitude, between 5 and 15 cm, as highlighted previously and a mean value of 16%. In position 1, but at the height of the DBH (Figures 6e and 6f), there is a high resistivity (values greater than 700  $\Omega$ m) and a low mechanical wave propagation velocity (approximately 500 m/s), corresponding to a low amplitude of the resistograph with 18% of mean value,

falling to 5%, between 7 and 11 cm. Also, between 7 and 11 cm, but in position 8 of the DBH, there is a decrease in the amplitude of the resistograph, falling from 30% to 15% and presenting the same characteristics of the ER and velocities of position 1.

The results of the *munguba* trunk assessment are presented below. Figure 7 shows the trunk sections obtained for the *munguba* MG1, which does not present any apparent external defect. Electrical resistivity varied between 9 and 260  $\Omega$ m, with lower values compared to eucalyptus specimens, which is related to its low density (Ganthaler et al., 2019). At the tree base (Figures 7a and 7b), the central region of the trunk with high resistivity and intermediate tomography velocity propagation (1245 m/s) stands out, not indicating an internal lesion. Likewise, for DBH, electrical resistivity (Figure 7c) and velocities (Figure 7d) did not present large variations.

The regions with the greatest variations in velocities shown by the tomography, analyzes were carried out with the resistograph (Figure 8), at point 5 at the base and at points 2 and 4 at the DBH. Due to the low density that the species presents, the values of resistance to drill penetration did not exceed 18%, showing a very soft wood, with mean values of 10%, 10% and 8%, respectively. In all results, from 3 cm onwards, the resistance curve reaches the level of 12% for the base and DBH (position 2), Figures 8a and 8d, respectively, and 10% for the DBH in position 4 (Figure 8g). The images overlapping with the resistography confirmed a homogeneous internal structure, confirming that the specimen did not present any damage.

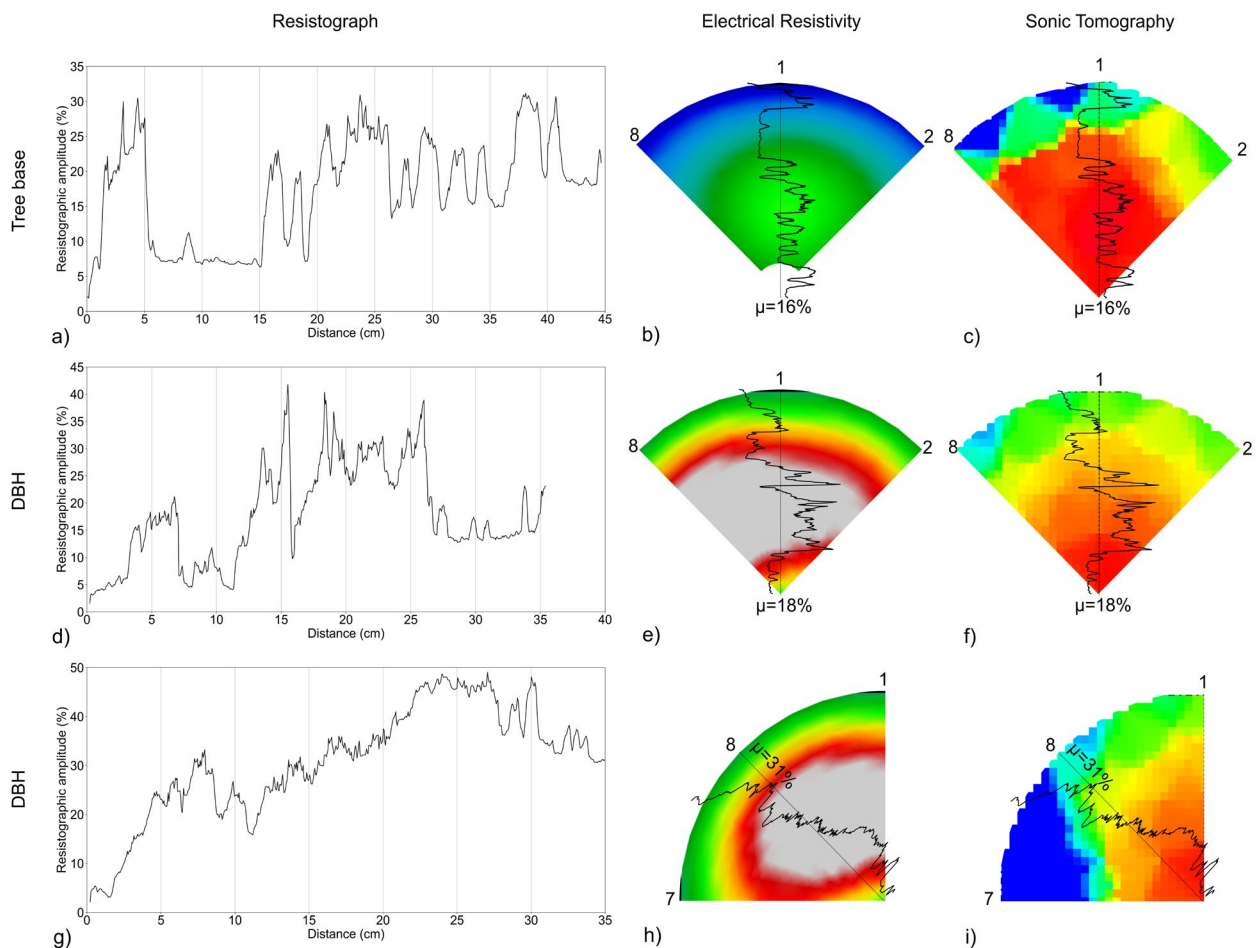


**Figure 6:** Resistograph results in eucalyptus EU2 compared with electrical resistivity and sonic tomography. a) Resistograph amplitudes in position 1, at the tree base. b) Overlap between electrical resistivity and resistographic amplitudes for the tree base. c) Overlap between sonic tomography and resistographic amplitudes for the tree base. d) Resistograph amplitudes in position 1, at the DBH. e) Overlap between electrical resistivity and resistographic amplitudes in position 1 for the DBH. f) Overlap between sonic tomography and resistographic amplitudes in position 1 for the DBH. g) Resistograph amplitudes in position 8, at the DBH. h) Overlap between electrical resistivity and resistographic amplitudes in position 8 for the DBH. i) Overlap between sonic tomography and resistographic amplitudes in position 8 for the DBH.

## DISCUSSION

By visual analysis (qualitative) of the images of the sections generated in *Eucalyptus* and *munguba*, there was a direct correlation between the methodologies employed (ER and tomography), mainly in eucalyptus. In two cases, the tomography showed a small variation in velocities, as in EU1 and MG1, due to some modification in the wood only, showing that in fact these specimens are intact, while in EU2, there was a significant alteration, showing a more accentuated decay, confirmed by resistography.

For electrical resistivity, the sections are consistent with what was expected, with lower values close to the bark due to sap flow and higher values in the heart of the tree, which is drier and does not transport water. Change regions consistent with tomography were identified, as in the DBH of eucalyptus EU1 and in both heights of EU2.

Each methodology uses a different physical property to characterize the same medium. In this way, it is also necessary to analyze the values found (quantitative analysis) for each method and verify if there is any kind of relationship between them. Table 1 presents the maximum and minimum values, at each evaluated height, of the propagation velocity of the mechanical wave and of the electrical resistivity obtained by the electrical resistivity method. In the cases analyzed, the greatest variation occurred in DBH of eucalyptus EU1 and the smallest in the tree base of *munguba* MG1.

Considering the difference between the densities of the two species, the average velocity propagation shows a little variation, with approximately 1100 m/s for eucalyptus and 1950 m/s for *munguba*. Electrical resistivity, on the other hand, showed the opposite behavior, with the average resistivity of eucalyptus greater (800  $\Omega\text{m}$ ) compared to *munguba* (200  $\Omega\text{m}$ ).

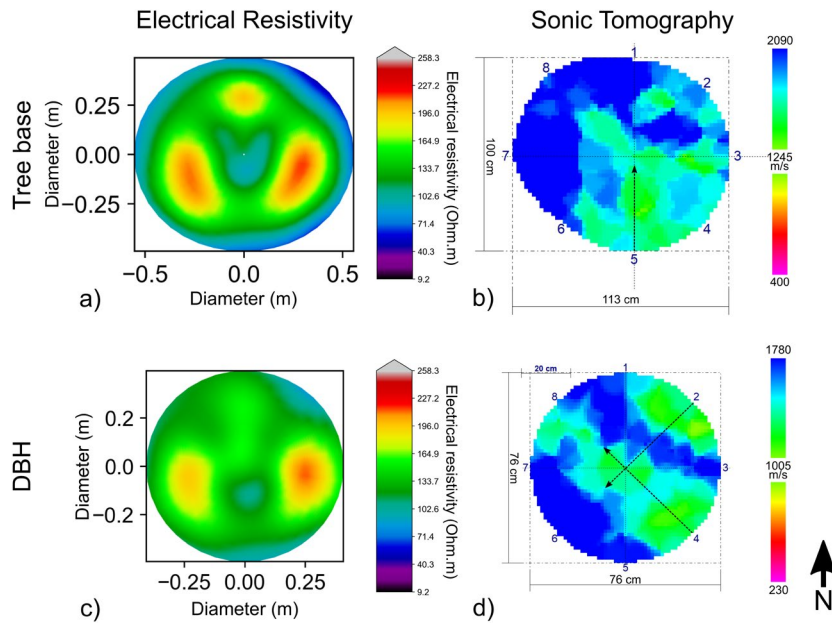


**Figure 7:** Results of the trunk analysis of *munguba* MG1 (at the tree base at 0.10 m height and at the DBH at 1.30 m height) with electrical resistivity and sonic tomography (black dashed line: position of the resistography data acquisition). a) Electrical resistivity at the tree base. b) Sonic tomography at the tree base. c) Electrical resistivity in the DBH. d) Sonic tomography in DBH.

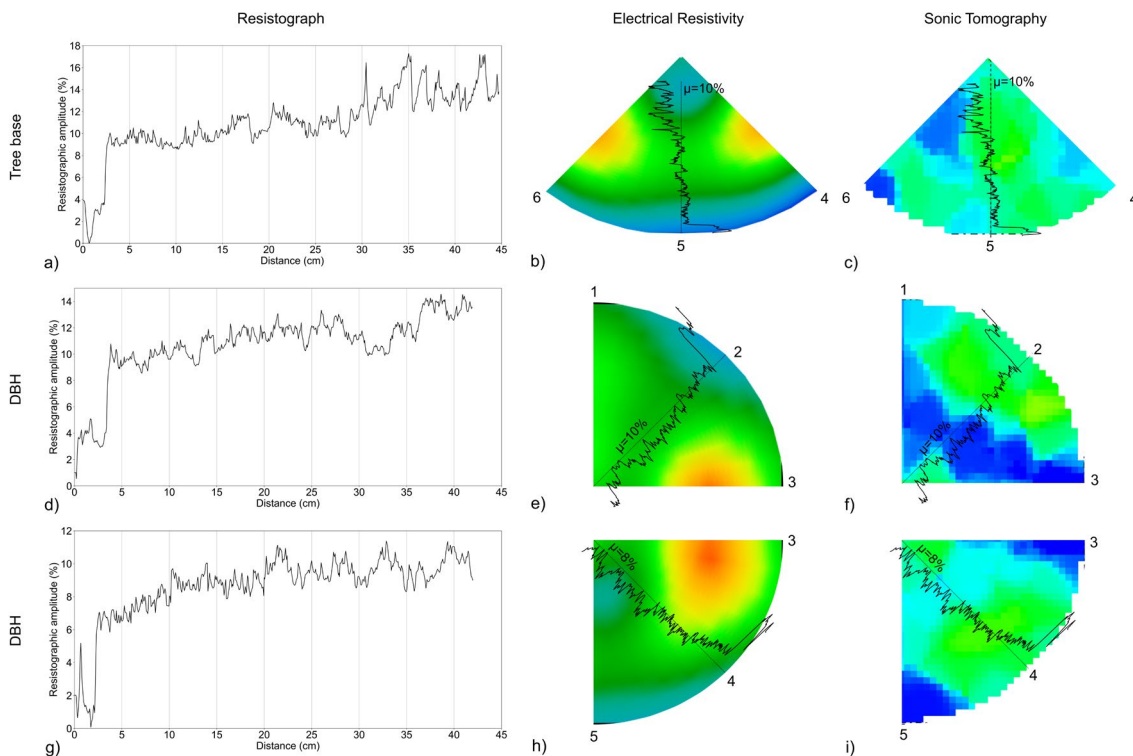


**Figure 8:** Resistograph results in *eucalyptus* MG1 compared with electrical resistivity and sonic tomography. a) Resistograph amplitudes in position 5, at the tree base. b) Overlap between electrical resistivity and resistographic amplitudes for the tree base. c) Overlap between sonic tomography and resistographic amplitudes for the tree base. d) Resistograph amplitudes in position 2, at the DBH. e) Overlap between electrical resistivity and resistographic amplitudes in position 2 for the DBH. f) Overlap between sonic tomography and resistographic amplitudes in position 2 for the DBH. g) Resistograph amplitudes in position 4, at the DBH. h) Overlap between electrical resistivity and resistographic amplitudes in position 4 for the DBH. i) Overlap between sonic tomography and resistographic amplitudes in position 4 for the DBH.

**Table 1:** Minimum and maximum velocity ( $v$ ) and electrical resistivity ( $\rho$ ) values in the analyzed specimens.

	Min. $v$ (m/s)	Max. $v$ (m/s)	Min. $\rho$ ( $\Omega$ m)	Max. $\rho$ ( $\Omega$ m)
EU1 basis	800	1440	54	590
EU1 DBH	925	2470	500	2907
EU2 basis	475	1480	65	402
EU2 DBH	600	1420	320	697
MG1 basis	1245	2090	40	220
MG1 DBH	1005	1780	100	200

## CONCLUSIONS

This work aimed to present and check the geophysical method of electrical resistivity through longitudinal profiles and validate the results with mechanical wave tomography and resistography in the evaluation of tree trunks. Data were acquired on two *Eucalyptus sp.* and one *Pachira aquatica* trunks, healthy and with internal problems, with tomography and electrical resistivity sections at the base and height of the DBH (1.30 m) and the results measured with the resistograph. Through the qualitative analysis, there was agreement between the images generated by the two methodologies, mainly for eucalyptus. Through the quantitative analysis, the values found for the bark and heartwood region are in accordance with the plant physiology, with increasing values towards the center of the trunk, and it was possible to correlate the values with the densities of the evaluated species. Thus, electrical resistivity proved to be a promising methodology for the internal analysis of tree trunks, showing its potential to correlate with the internal water content of the trunk, in addition to being able to characterize the presence of hollow regions more accurately. Despite this, it is necessary to carry out more data acquisitions in other species and in more specimens to obtain an accurate evaluation of the methodology.

## AUTHORSHIP CONTRIBUTION

Project Idea: VRNS; MFC

Database: VRNS; MFC

Processing: VRNS; MFC; BAFM

Analysis: VRNS; BAFM; JVFL; MFC

Writing: VRNS; BAFM; JVFL; MFC

Review: VRNS; BAFM; JVFL; MFC

## ACKNOWLEDGMENTS

Funding: This work was supported in part by São Paulo Reserach Foundation FAPESP (Grant: 2017/22855-9 and 2019/09483-0). VRNS also thanks the postgraduate course in Urban Forestry at UFRRJ.

## REFERENCES

- APAYDIN, O.; ISSEVEN, T.; CITIR, Y.; et al. Extracting tomographic images of interior structures of cylindrical objects and trees using Ground Penetrating Radar method. *Results in Engineering*, v. 14, 2022.
- BALAWANT, P.; JYOTHI, V.; PUJARI, P. R.; et al. Tree root imaging by electrical resistivity tomography: geophysical tools to improve understanding of deep root structure and rhizospheric processes. *Tropical Ecology*, v. 63, p.319-324, 2022.
- BURCHAM, D. C.; BRAZEE, N. J.; MARRA, R. E.; et al. Geometry matters for sonic tomography of trees. *Trees*, v. 37, p. 837-848, 2023.
- CARVALHO, T. S.; MARTINI, A.; SOUZA, M. M.; et al. O efeito de rajadas de vento na inclinação da placa de raízes em árvores urbanas. *Revista de Gestão Ambiental e Sustentabilidade*, v. 13, n. 1, 2023.
- CAVALARI, A. A.; VELASCO, G. D. N.; SILVA-LUZ, C. L.; et al. Predicting tree failure to define roles and guidelines in risk management, a case study in São Paulo/Brazil. *Urban Forestry and Urban Greening*, v. 91, 2024.
- CRUZ, E. D. Germinação de sementes de espécies amazônicas: mamorana (*Pachira aquatica* Aubl.). *Comunicado Técnico 337*, Embrapa, 2022.
- CUNHA, V. L. C. M.; MAGALHÃES, L. M. S.; FREITAS, W. K.; et al. Conflitos da arborização com elementos urbanos na cidade de Valença, Estado do Rio de Janeiro. *Revista da Sociedade Brasileira de Arborização Urbana*, v. 15, n. 2, p. 28-41, 2020.
- DEFLORIO, G.; FINK, S.; SCHWARZE, F. W. M. R. Detection of incipient decay in tree steams with sonic tomography after wounding and fungal inoculation. *Wood Science Technology*, v. 42, p. 117-132, 2008.
- DUDKIEWICZ, M.; DURLAK, W. Sustainable management of very large trees with the use of acoustic tomography. *Sustainability*, v. 13, n. 21, 2021.
- EHOSIOKE, S.; NGUYEN, F.; RAO, S.; et al. Sensing the electrical properties of roots: A review. *Vadoze Zone Journal*, v. 19, n. 1, e20082, 2020.
- EMERICK, T. G. Risco de queda de árvores urbanas: a associação entre os parâmetros da análise visual, tomogramas e ocorrência de queda. *Dissertação apresentada à Universidade Federal de Viçosa*, 135p, 2021.
- FENG, D.; LIU, Y.; WANG, X.; et al. Quantitative evaluation for the internal defects of tree trunks based on the wavefield reconstruction inversion using Ground Penetrating Radar data. *Forest*, v. 14, n.5, 2023.
- FU, Q.; QIU, E.; ZHANG, Y.; et al. Mechanisms of trunk cavity formation of large old trees in urban landscapes: A case study on four tree species in Beijing. *Ecological Indicators*, v. 158, e111388 2024.
- GÖCKE, L.; RUST, S.; WEIHS, U.; et al. Combining sonic and electrical impedance tomography for the nondestructive testing of trees. 15<sup>th</sup> International Symposium on Nondestructive Testing of Wood, Duluth, Minnesota, USA, September 10-12, 2008.
- GROTE, R.; SAMSON, R.; ALONSO, R.; et al. Functional traits of urban trees: air pollution mitigation potential. *Frontiers in Ecology and the Environment*, v. 14, n. 10, p. 543-550, 2016.
- GUARDIA, I. Velocidade de onda mecânica na avaliação de raízes de arborização de árvores nas cidades. *Dissertação de Mestrado defendida em Escola Superior de Agricultura Luiz de Queiroz, Universidade de São Paulo*, 164p, 2020.

- HAGREY, A. S. Electrical resistivity imaging of tree trunks. *Near Surface Geophysics*, v.4, n.3, p. 179-187, 2006.
- KANTAVICHAI, R.; TURNBLOM, E. C. Identifying non-thrive trees and predicting wood density from resistograph using temporal convolution network. *Forest Science and Technology*, v. 18, n.4, 2022.
- LARSSON, B.; BENGSSON, B.; GUSTAFSSON, M. Nondestructive detection of decay in living trees. *Tree Physiology*, v. 24, n.7, p. 853-857, 2004.
- NOWAK, D. J. Understanding i-Tree: 2021 Summary of Programs and Methods. U.S. Department of Agriculture, Forest Service, Appendix 11: Wood Density Values, 2021.
- ORELLANA, E. *Prospeccion Geoelectrica en Corriente Continua*. Ed. Paraninfo, Madrid, 523p., 1972.
- PAPANDREA, S. F.; CATALO, M. F.; ZIMBALATTI, G. et al. Comparative evaluation of inspection techniques for decay detection in urban trees. *Sensors and Actuators: A. Physical*, v. 340, e113544, 2022.
- RAHMAN, M. A.; MOSER, A.; GOLD, A.; et al. Vertical air temperature gradients under the shade of two contrasting urban tree species during different types of summer days. *Science of the Total Environment*, v. 633, p. 100-111, 2018.
- REYNOLDS, J. M. *An introduction to applied and environmental geophysics*. John Wiley; Sons Ltd., 806p., 1997.
- RINN, F. Resistographic visualization of tree-ring density variations. *International conference tree rings and environment*, Tucson, AZ, 1994.
- RINN, F.; SCHWEINGRUBER, F. -H., SCHÄR, E. Resistograph and x-ray density charts of wood: comparative evaluation of drill resistance profiles and x-ray density charts of different wood species. *Holzforschung*, v. 50, n.4, p. 303-311, 1996.
- RUST, S.; GÖCKE, L. A new tomographic device for the non-destructive testing of standing trees. In: *Proceedings of the 12th International Symposium on Nondestructive Testing of Wood*. University of Western Hungary, Sopron, 13 - 15 September 2000, 233 – 238, 2000.
- SANTOS, N. R. Z.; TEIXEIRA, I. F. *Arborização de vias públicas: ambiente x vegetação*, 1ª Ed. Gráfica Editora Palloti, Porto Alegre-RS, 2001.
- SANTOS, V. R. N.; CAETANO, M. F.; MARTINATTI, M.; et al. Tecnologia ANDAS para mapeamento 3D do sistema radicular de árvores utilizando georadar e eletrorresistividade. *Revista da Sociedade Brasileira de Arborização Urbana*, v. 17, n. 1, p. 17-36, 2022.
- Secretaria Municipal do Verde e do Meio Ambiente *Manual Técnico de Arborização Urbana*. 124p, 2015.
- SMULSKI, S. J. Relationship of stress wave and static bending determined properties of four northeastern hardwoods. *Wood and Fiber Science*, v. 23, n. 1, p. 44-57, 1991.
- SOGE, A. O.; POPOOLA, O. I.; ADETOYINBO, A. A. A four-point electrical resistivity method for detecting wood decay and hollows in living trees. *European Journal of Wood and Wood Products*, v. 77, p. 465-474, 2019.
- SUCHOCKA, M.; JELONEK, T.; BLASZCZYK, M.; et al. Risk assessment of hollow-bearing trees in urban forests. *Scientific Reports*, v. 13, 2023.
- TELFORD, W. M.; GELDART, L. P., SHERIFF, R. E. *Applied Geophysics*. Second Edition, Cambridge University Press, United Kingdom, 770p., 1990.
- TUDO, C.; YAMASE, K.; IKENO, H.; et al. Maximum Rooting Depth of *Pinus thunbergii* Parl. Estimated with Depth at the Center Point of Rotation in a Tree-Pulling Experiment in a Coastal Forest in Japan. *Forests*, v. 13, n.9, p.1506, 2022.
- VOGT, J.; GILLNER, S.; HOFMANN, M.; et al. Citree: A database supporting tree selection for urban areas in temperate climate. *Landscape and Urban Planning*, v. 157, p. 14-25, 2017.